High-fidelity Noncovalent Synthesis of Hydrogen-bonded Macrocyclic Assemblies

Carlos Montoro-García, Jorge Camacho-García, Ana M. López-Pérez, Nerea Bilbao, Sonia Romero-Pérez, María J. Mayoral and David González-Rodríguez*

Abstract: A hydrogen-bonded cyclic tetramer is assembled with remarkably high effective molarities from a properly designed dinucleoside monomer. This self-assembled species exhibits an impressive thermodynamic and kinetic stability and is formed with high fidelities within a broad concentration range.

Noncovalent synthesis comprises the spontaneous generation of a well-defined structure from a set of molecular components bound by supramolecular interactions.[1] The understanding and application of this concept to discrete macrocyclic architectures is very appealing, not only because of their stimulating structure, but also because of their manifold possibilities.[2] Self-assembled macrocycles[3] offer low synthetic efforts and high versatilities but,[2a,4] as they are built from the interplay of multiple weak interactions operating under thermodynamic equilibrium, they do not enjoy the persistency and robustness of their covalent analogues. Besides, achieving complete selectivity (i.e. high fidelity) towards the target cyclic structure is a challenging task that demands careful molecular design.

Key in this design is the optimization of chelate cooperativity,[5] which is also responsible for many of the "all-or-nothing" molecular assembly processes in biological systems.[6] It originates from the fact that an intramolecular association event (i.e. ring closure) is favoured over an intermolecular one because it does not involve a high translational and rotational entropy loss. The equilibrium constant ratio K_{intra}/K_{inter} is defined as the effective molarity (*EM*) of the system,[7] and is used to quantify the chelate effect.[8] The maximization of *EM* for a given macrocycle is therefore essential to reach high yields over "open" oligomers, on one hand, and over other undesired cyclic structures, on the other (Figure 1a).[9] The enthalpic term of *EM* is mainly correlated with the strain generated upon cyclization and can be thus optimized by preorganization of the monomer structure so that the binding interaction produces the target cyclic assembly devoid of strain. The entropic term encompasses the loss of conformational degrees of freedom upon cyclization and is often related to the number and nature of rotatable bonds present in the monomer. Hence, rigid monomers with low conformational freedom are preferable. Entropy is also responsible for the notable decay in *EM* values as the cyclic assembly is built from more molecules.

Here, we focus on the study of a ditopic monomer (**GC**; Figure 1b) that has been designed to yield cyclic tetramer[10] H-bonded assemblies[11] with high *EM* values. **GC** comprises complementary guanosine (G) and cytidine (C) nucleosides[12] at both edges having bulky lipophilic groups at the ribose to afford solubility and prevent stacking,[13] so that we can only focus on the study of the H-bonding process in solution. It is essential to note that, upon Watson-Crick pairing, the 5-C position and the 8-G position form an angle of 90º. We have linked those positions in **GC** through a rigid, linear and π-conjugated *p*-diethynylbenzene block, so that triple H-bonding interactions between complementary bases afford an unstrained square-shaped assembly (*c***GC**$_4$) with minimal entropic cost. In this work, we have devised several experiments that demonstrate the consequences of a suitable monomer design in the fidelity of the self-assembly process and in the thermodynamic and kinetic stability of ring-closed structures when compared to linear assemblies.

Figure 1. (**a**) Self-assembly of a ditopic monomer (**GC**) to yield cyclic (*c***GC**$_4$) or

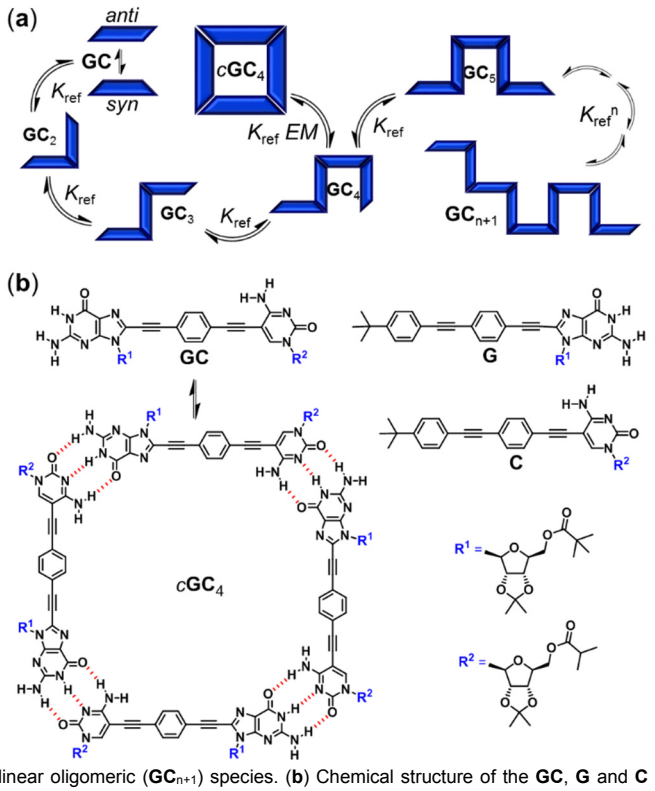

linear oligomeric (**GC**$_{n+1}$) species. (**b**) Chemical structure of the **GC**, **G** and **C** compounds studied in this work,[14] as well as the cyclic tetramer *c***GC**$_4$.

The ^{1}H NMR spectra of **GC** in chlorinated solvents displayed a single set of proton resonances that are characteristic of G-C association (Figure 2a). The H-bonded G-H^1 amide and the C-H^2 amine signals are found at 13.4 and 10.0, respectively. The C-H^3 signal was found around 8-6 ppm, depending on the solvent used (Figure S1). On the other hand, the G-amine protons are found

C. Montoro-García, J. Camacho-García, Dr. A. M. López-Pérez, N. Bilbao, S. Romero-Pérez, Dr. M. J. Mayoral, Dr. D. González-Rodríguez
Nanostructured Molecular Systems and Materials group
Departamento de Química Orgánica, Facultad de Ciencias, Universidad Autónoma de Madrid, 28049 Madrid, Spain
E-mail: david.gonzalez.rodriguez@uam.es

Supporting information for this article is given via a link at the end of the document.

as a broad coalesced signal at 298 K that splits in two sharp signals at 8.5 (H^4) and 5.4 (H^5) ppm below 273 K (Figures 2a and S2).[15] Mono- and bidimensional NOE experiments (Figures 3b and S3) showed cross-peaks between the H-bonded G-H^1 and C-H^2 protons, hence confirming G-C association.

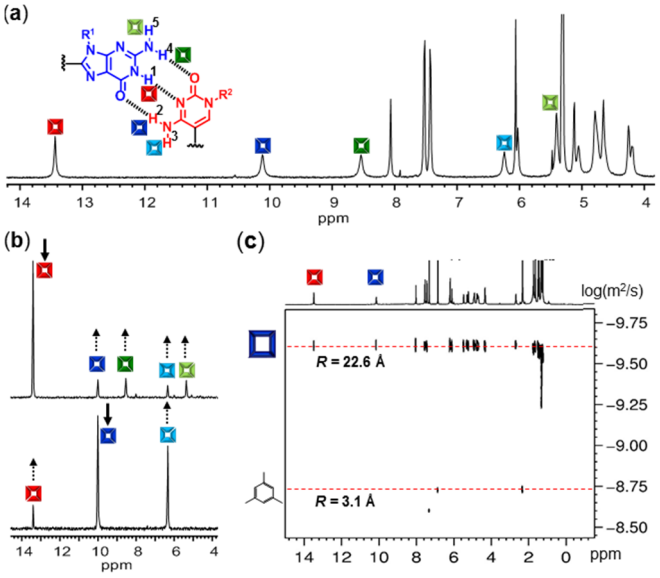

Figure 2. (**a**) ^{1}H NMR spectrum of **GC** in CD_2Cl_2 at 248 K showing all the amide and amine proton signals. (**b**) 1D NOE spectra of **GC** in $CDCl_3$ at 298 K irradiating the G-H^1 signal (top) or the C-H^2 signal (bottom). (**c**) DOSY NMR spectrum of **GC** in $CDCl_3$ at 298 K. In all cases, $C = 10^{-2}$ M.

It is interesting to note that the shape and position of the H-bonded G-H^1 and C-H^2 proton signals in **GC** are virtually not sensitive to concentration (10^{-1}–10^{-4} M; Figure S4), temperature (223–373 K; Figure S2) or solvent changes ($CDCl_3$, CD_2Cl_2, $CDCl_2CDCl_2$, THF-D_8, acetone-D_6; Figure S1). This is in sharp contrast to the behavior of the **G-C** 1:1 complex, whose signals are quite sensitive to these experimental changes, and suggests that a particularly stable supramolecular entity is formed by **GC**. In accordance, DOSY experiments in $CDCl_3$ within the 10^{-2} M to 10^{-4} M concentration range suggested the presence of a single species with a diffusion coefficient that is consistent with the hydrodynamic radius expected for ***c*GC$_4$** (Figures 2c and S5). ESI Q-TOF mass spectrometry experiments also sustained the formation of a tetramer (Figure S6), and we could detect the single, double and triple-charged **GC$_4$** peaks and some of its fragments.[14]

In order to shed more light into the structural nature and the thermodynamic and kinetic characteristics of ***c*GC$_4$** in solution, we devised several experiments aimed to dissociate it. Due to its unusual stability, when compared for instance with the **G-C** 1:1 pair, we employed three drastic approaches: a) the use of very polar solvents in NMR experiments, such as DMSO-D_6 of DMF-D_7, which are able to strongly compete for H-bonding; b) optical spectroscopy experiments at very low concentrations and; c) competition experiments with mononucleoside stoppers.[13]

In contrast to the NMR solvents previously mentioned, the ^{1}H NMR spectrum of **GC** in DMSO-D_6 exhibited G-H^1 and C-H^2 proton signals at 10.8 and 7.9 ppm, attributed to the solvent-bound **GC** monomer. The increase of the DMSO content in $CDCl_3$–DMSO-D_6 solvent mixtures resulted in the progressive dissociation of ***c*GC$_4$**. However, 3 main points should be remarked in these experiments that differ significantly from the behavior of the **G-C** 1:1 complex (Figures 3a and S7): 1) the associated ***c*GC$_4$** can resist large amounts of DMSO (it persists even at 80% v/v), which is quite notable for a H-bonded assembly; 2) the monomer-tetramer exchange seems to be very slow in the NMR timescale in these conditions, since the shape and position of all signals do not change throughout the whole experiment and; 3) an all-or-nothing behavior was noted, meaning that no other intermediate supramolecular species was detected (it is either ***c*GC$_4$** or **GC**, but nothing else). In DMF-D_7 a similar behavior was observed, but

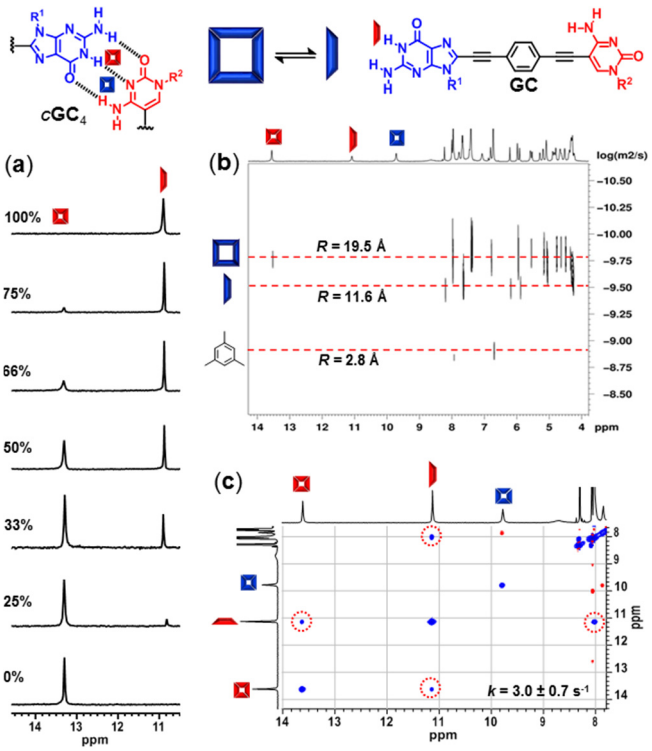

dissociation was not completed even in 100% DMF-D_7.[14]

Figure 3. (**a**) Amide region of the ^{1}H NMR spectrum of **GC** in $CDCl_3$-DMSO-D_6 solvent mixtures as a function of the DMSO content (v/v %), showing ***c*GC$_4$** dissociation (**b**) DOSY NMR spectrum of **GC** in DMF-D_7 showing the **GC** and ***c*GC$_4$** signals with different diffusion coefficients. (**c**) Amide region of the EXSY spectrum of **GC** in DMF-D_7 at a 200 ms mixing time. $C = 10^{-2}$ M; $T = 298$ K.

At a 10^{-2} M **GC** concentration, the use of a 1:1 $CDCl_3$-DMSO-D_6 mixture or pure DMF-D_7 resulted in an approximately 1:1 **GC**–***c*GC$_4$** equilibrium mixture that was studied further. DOSY experiments indicated now the presence of two diffusing species (Figures 3b and S8): one of them assigned to ***c*GC$_4$**, with lower diffusion coefficients, and the other one to the **GC** monomer. The **GC**–***c*GC$_4$** exchange kinetics was studied by EXSY in DMF-D_7 (Figures 3c and S9). From these experiments we could calculate the exchange rate constant ($k = 3.0 \pm 0.7$ s^{-1}), and hence confirm that the **GC**–***c*GC$_4$** exchange is remarkably slow even in this polar solvent, which underlines the high kinetic stability of the cyclic ensemble. On the other hand, in dilution experiments from 10^{-1} to

10^{-4} M (Figure S10) or in cooling experiments from 323 to 273 K (Figure S11) we could monitor the **GC**–*c***GC**$_4$ equilibrium. Again, no sign of any other species was found in these experiments, highlighting the cooperative nature of the cyclic assembly process. Since the exchange is very slow, we could derive the equilibrium constants (K_T) by signal integration (Table 1), and confirm that a tetramerization process holds for the whole range of concentrations and temperatures in both polar solvent systems.[16] A Van´t Hoff analysis of the temperature-dependent data afforded the thermodynamic parameters ΔH and ΔS (Table 1).

A second method we devised to study the **GC**–*c***GC**$_4$ equilibrium was the use of lower concentrations (10^{-4}–10^{-6} M) and more sensitive techniques like absorption, emission and circular dichroism (CD) spectroscopy as a function of concentration and temperature (Figure 4). Here, the choice of solvent was critical (Figure S12). We found that solvents of intermediate polarity, like THF or dioxane,[14] are ideal media to study these equilibria.

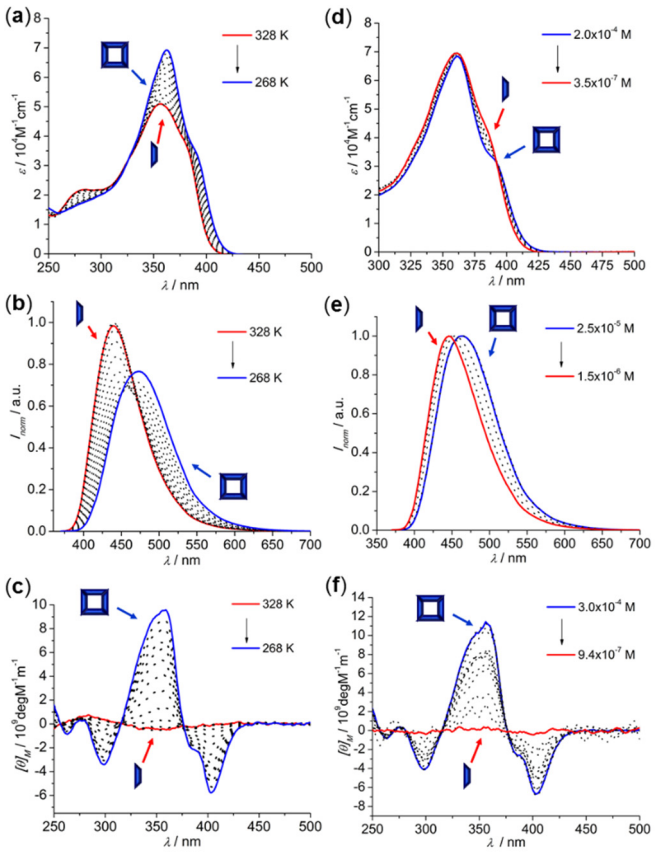

Figure 4. Absorption (**a**,**d**), emission (**b**,**e**) and CD changes (**c**,**f**) of **GC** in THF with temperature (**a**-**c**; C = 1.25x10^{-5} M) or concentration (**d**-**f**; T = 298 K). Insets: fitting of the changes at (**a**) 400, (**b**) 439 and (**c**) 404 nm to the equal-K model.

When the chiral monomers associate in a cyclic tetramer assembly at high concentrations or low temperatures, a red-shifted absorption shoulder at 393 nm, red-shifted emission maxima and, significantly, a Cotton CD effect arising with maxima at 357 and minima at 299 and 404 nm were evidenced. Both temperature- and concentration-dependent data were fitted to suitable models[14] in order to obtain the relevant thermodynamic parameters in THF (K_T, ΔH and ΔS; see Figure S13 and Table 1).

Finally, a third way we employed to study *c***GC**$_4$ dissociation consists in the addition a competitor for H-bonding. We know so far that the **GC**–*c***GC**$_4$ equilibrium is very slow and shifted to the tetramer. Now, if we add increasing amounts of **C**, it will compete with the **GC** monomer for binding to the G units in *c***GC**$_4$, which will gradually shift the equilibrium towards a **GC·C** complex. We were able to monitor this competition at different **GC** concentrations in $CHCl_3$, THF and DMF by both ^{1}H NMR and fluorescence titration experiments (Figure 5).

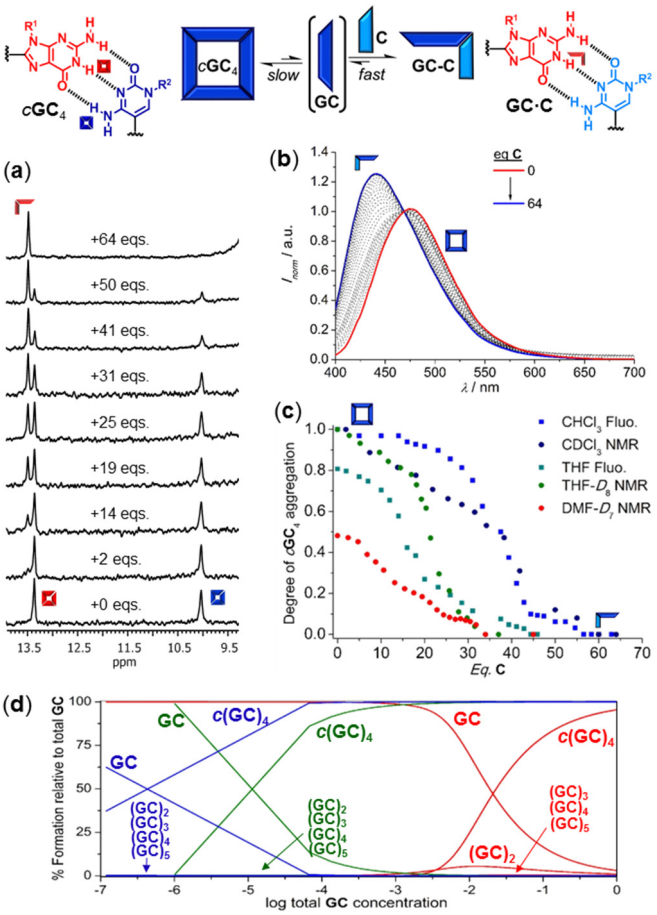

Figure 5. Titration experiments of **GC** with **C** at 298 K. (**a**) ^{1}H NMR changes (C = 10^{-3} M) in $CDCl_3$. (**b**) Normalized Fluorescence emission changes (C = 5 x 10^{-5} M; λ_{exc} = 390 nm) in $CHCl_3$. (**c**) Plots of the degree of *c***GC**$_4$ association, measured by ^{1}H NMR or emission, as a function of the equivalents of **C** added. (**d**) Speciation profiles including the **GC**, **GC**$_2$, **GC**$_3$, **GC**$_4$, **GC**$_5$ and *c***GC**$_4$ species. Solvent codes (for **c**,**d**): DMF (red), THF (green) and $CHCl_3$ (blue).

As evidenced in ^{1}H NMR titrations (Figures 5a and S14), the addition of **C** to a solution of *c***GC**$_4$ results in the gradual disappearance of the *c***GC**$_4$ proton signals and the emergence of a new set of signals attributed to the **GC·C** complex, in fast equilibrium with excess **C**. It is significant to note again that *c***GC**$_4$ is in slow exchange with the other species in solution, which allowed us to withdraw their relative concentrations by integration. In emission experiments (Figure 5b and S14), a blue shift was monitored as *c***GC**$_4$ is dissociated with excess **C**. Actually, in these

experiments the intra- and intermolecular G-C binding events are made to compete, so we could directly withdraw K_T from the relevant equilibrium constants (Table 1).[14] Figure 5c shows the competition trends in the three solvents. In order to fully dissociate *c***GC**$_4$ one must reach *ca.* 60 ($CHCl_3$), 40 (THF) or 35 (DMF) **C** equivalents,[18] which underlines the stability of the cyclic assembly.

From the different K_T values obtained and the reference G-C association constants (K_{ref}), determined by titration experiments with **G** and **C** (Figure S15), we could estimate the *EM* in each of the 3 solvents employed (Table 1) using the relationship: $K_T = K_{ref}^4 \cdot EM$.[17] The product $K_{ref} \cdot EM$ is considerably enhanced in low polarity media and in all cases exceeds $185 \cdot n$, (*n* being the number of monomers in the cycle; *n* = 4), a condition defined by Ercolani to reach complete cycle assembly at a given monomer concentration.[8b] The speciation profiles simulated in each solvent (Figure 5d) reproduce satisfactorily our experimental results and illustrate that *c***GC**$_4$ can be formed quantitatively in a wide range of concentrations, as long as the binding constant is kept high enough by low solvent competition for G-C H-bonding. The lower self-assembly concentration (*Isac*),[8b] that is, the concentration at which half of the monomer is assembled into macrocycles, was estimated as: $Isac^{DMF}$ = 1.6 x 10^{-2} M, $Isac^{THF}$ = 9.5 x 10^{-4} M, and $Isac^{CHCl3}$ = 4.1 x 10^{-7} M (see also Figure 5d).[14]

Table 1. Thermodynamic parameters obtained for the **GC** tetramerization process in different solvents.

solvent	K_{ref} M^{-1}	K_T M^{-3}	*EM* M	ΔH $kJmol^{-1}$	ΔS $Jmol^{-1}K^{-1}$
DMF	5.7±0.3 [a]	2.3±0.8 x10^5 [c]	218	-155±38 [h]	-425±94 [h]
		3.8±2.4 x10^5 [d]	357		
THF	1.5±0.1 x10^3 [a]	1.0±0.2 x10^{15} [e]	197	-225±44 [f]	-465±126 [f]
		2.2±1.8 x10^{15} [f]	434		
		2.7±1.5 x10^{15} [d]	526		
		2.1±0.3 x10^{15} [g]	414		
$CHCl_3$	2.8±0.3 x10^4 [b]	5.6±3.1 x10^{20} [d]	910		
		5.0±0.1 x10^{20} [g]	813		

[a] Titration with **G** and **C** (Figure S15). [b] Determined in ref 13. [c] Dilution in DMF-D_7 (Figure S10). [d] NMR competition (Figure S14). [e] Dilution in THF (Figure S13). [f] Temperature experiments in THF (Figure S13). [g] Fluorescence competition (Figure S14). [h] Temperature experiments in DMF-D_7 (Figure S11).

This work reveals the consequences of optimal monomer design on the fidelity of a supramolecular oligomerization process towards a specific macrocyclic structure. *c***GC**$_4$ exhibits an impressive thermodynamic stability and constitutes a kinetically steady product in the overall self-assembly landscape *even in highly polar solvents*, where H-bonded association is typically too weak. Both monomer structure and binding interaction geometry and nature have to be considered in order to produce cyclic species devoid of strain and with minimal conformational entropy loss. This was achieved on one hand employing a rigid monomer with only 4 rotatable linear π-conjugated bonds. Rotation around these bonds, however, is not restrained upon self-assembly. The only degree of freedom that is lost upon cycle formation, when compared to open oligomers, is the relative conformational arrangement between nucleobases. *c***GC**$_4$ demands all Watson-Crick edges to be in a *syn* conformation but an open structure is free to alternate between *anti* and *syn* conformations (see Figure 1). On the other hand, *c***GC**$_4$ assembles through a triple H-bonding interaction that is relatively strong and asymmetric (DDA-AAD pattern), and directs association with a well-defined 90º angle. We believe that the rigidity and non-rotatable nature of this multipoint binding interaction is a key factor that notably increases the magnitude of *EM* in *c***GC**$_4$ (10^2–10^3 M)[17,18] when compared to other cyclic tetramers based on metal-ligand interactions (*EM* = 0.1–20 M).[10] Our results underscore the use of multiple H-bonding interactions, in this case DNA bases, to enhance chelate cooperativity in order to produce a target assembly with high fidelity.

Acknowledgements

Funding from MINECO (*CTQ2011-23659*) and the E.U. (*ERC-Starting Grant 279548*) is gratefully acknowledged.

Keywords: Supramolecular Chemistry • Noncovalent Synthesis • Chelate Effect • Nucleoside Self-assembly • Effective Molarity

[1] a) L. J. Prins, D. N. Reinhoudt, P. Timmerman, *Angew. Chem. Int. Ed.* **2001**, *40*, 2382–2426; *Angew. Chem.* **2001**, *113*, 2446–2492.

[2] a) M. Iyoda, J. Yamakawa, M. J. Rahman, *Angew. Chem. Int. Ed.* **2011**, *50*, 10522–10553; *Angew. Chem.* **2011**, *45*, 10708–10740.

[3] P. Ballester, J. de Mendoza in *Modern Supramolecular Chemistry* (Eds.: F. Diederich, P. J. Stang, R. R. Tykwinski), Wiley-VCH, Weinheim, 2008, 69-111.

[4] S. Höger, *Angew. Chem. Int. Ed.* **2005**, *44*, 3806–3808; *Angew. Chem.* **2005**, *25*, 3872–3875.

[5] a) C. A. Hunter, H. L. Anderson, *Angew. Chem. Int. Ed.* **2009**, *48*, 7488–7499; *Angew. Chem.* **2009**, *41*, 7624–7635; b) G. Ercolani, L. Schiaffino, *Angew. Chem. Int. Ed.* **2011**, *50*, 1762–1768; *Angew. Chem.* **2011**, *8*, 1800–1807.

[6] Focus Issue on Cooperativity. *Nat. Chem. Biol.* **2008**, *4*, 433-507.

[7] L. Mandolini, *Adv. Phys. Org. Chem.* **1986**, *22*, 1–111.

[8] a) X. Chi, A. J. Guerin, R. A. Haycock, C. A. Hunter, L. D. Sarson, *J. Chem. Soc., Chem. Commun.* **1995**, 2563–2565; b) G. Ercolani, *J. Phys. Chem. B,* **1998**, *102*, 5699–5703; c) G. Ercolani, *J. Phys. Chem. B,* **2003**, *107*, 5052–5057; d) G. Ercolani, *Struct. Bond.* **2006**, *121*, 167–215.

[9] The influence of different factors on chelate cooperativity has been analyzed. See: a) C. A. Hunter, M. C. Misuraca, S. M. Turega, *J. Am. Chem. Soc.* **2011**, *133*, 20416–20425; b) M. C. Misuraca, T. Grecu, Z. Freixa, V. Garavini, C. A. Hunter, P. van Leeuwen, M. D. Segarra-Maset, S. M. Turega, *J. Org. Chem.* **2011**, *76*, 2723–2732; c) H. J. Hogben, J. K. Sprafke, M. Hoffmann, M. Pawlicki, H. L. Anderson, *J. Am. Chem. Soc.* **2011**, *133*, 20962–20969; d) C. A. Hunter, M. C. Misuraca, S. M. Turega, *Chem. Sci.* **2012**, *3*, 589–601; e) C. A. Hunter, M. C. Misuraca, S. M. Turega, *Chem. Sci.* **2012**, *3*, 2462–2469; f) H. Adams, E. Chekmeneva, C. A. Hunter, M. C. Misuraca, C. Navarro, S. M. Turega, *J. Am. Chem. Soc.* **2013**, *135*, 1853–1863; g) H. Sun, C. A. Hunter, C. Navarro, S. Turega, *J. Am. Chem. Soc.* **2013**, *135*, 13129–13141.

[10] For other cyclic tetramer assemblies whose *EM*s have been calculated, see: a) X. Chi, A. J. Guerin, R. A. Haycock, C. A. Hunter, L. D. Sarson, *J. Chem. Soc., Chem. Commun.* **1995**, 2567–2569; c) G. Ercolani, M. Ioele, D. Monti, *New J. Chem.* **2001**, *25*, 783–789; d) I.-W. Hwang, T. Kamada, T. K. Ahn, D. M. Ko, T. Nakamura, A. Tsuda, A. Osuka, D. Kim, *J. Am. Chem. Soc.* **2004**, *126*, 16187–16198.

[11] For other H-bonded cyclic tetramer assemblies in solution, see: a) C. Nuckolls, F. Hof, T. Martín, Jr. J. Rebek, *J. Am. Chem. Soc.* **1999**, *121*,

10281–10285 b) H. Ohkawa, A. Takayama, S. Nakajima, H. Nishide, *Org. Lett.* **2006**, *8*, 2225–2228; c) E. Orentas, C.-J. Wallentin, K.-E. Bergquist, M. Lund, E. Butkus, K. Wärnmark, *Angew. Chem. Int. Ed.* **2011**, *50*, 2071–2074; *Angew. Chem.* **2011**. *9*, 2119–2122. d) Y. Yang, M. Xue, L. J. Marshall, J. de Mendoza, *Org. Lett.* **2011**, *12*, 3186–3189.

[12] For the use of nucleobases in supramolecular chemistry: a) S. Sivakova, S. J. Rowan, *Chem. Soc. Rev.* **2005**, *34*, 9–21; b) J. L. Sessler, C. M. Lawrence, J. Jayawickramarajah, *Chem. Soc. Rev.* **2007**, *36*, 314–325.

[13] J. Camacho-García, C. Montoro-García, A. M. López-Pérez, N. Bilbao, S. Romero-Pérez, D. González-Rodríguez, *Org. Biomol. Chem.* **2015**, DOI: 10.1039/C5OB00098J.

[14] See the Supporting information for further details.

[15] a) D. González-Rodríguez, J. L. J. van Dongen, M. Lutz, A. L. Spek, A. P. H. J. Schenning, E. W. Meijer, *Nature Chem.* **2009**, *1*, 151-155.; b) D. González-Rodríguez, P. G. A. Janssen, R. Martín-Rapún, I. De Cat, S. De Feyter, A. P. H. J. Schenning, E. W. Meijer, *J. Am. Chem. Soc.* **2010**, *132*, 4710-4719.

[16] Cyclic trimer or pentamer assemblies were not properly fitted by the different methods employed in this work. Molecular modeling studies at the PM3 level (Figure S5) show that these structures are more strained and far from achieving an optimal G-C H-bonding geometry. Moreover, cyclic tetramer assemblies were observed by STM studies over HOPG, which will be the subject of a forthcoming publication.

[17] The competition trends and the calculated *EM* values seem to reveal a relationship between *EM* and binding strength (K_{ref}), modulated by the solvent. Further studies will be performed in order to address this issue.

[18] To the best of our knowledge, this is the first example of a H-bonded cyclic tetramer whose *EM* values were calculated, so we could not make a direct comparison. A cyclic trimer assembled *via* double H-bonding interactions was reported to have *EM* values of 760 M. See ref. 3 and: S. C. Zimmerman, B. F. Duerr, *J. Org. Chem.* **1992**, *57*, 2215–2217. On the other hand, a related ethenylene-bound G-C monomer has been reported by the Sessler's group to produce instead trimeric macrocycles: J. L. Sessler, J. Jayawickramarajah, M. Sathiosatham, C. L. Sherman, J. S. Brodbelt, *Org. Lett.,* **2003**, *5*, 2627–2630.

Entry for the Table of Contents

COMMUNICATION

Fine design of a dinucleoside monomer leads to H-bonded macrocyclic tetramer assemblies with high effective molarities and remarkable thermodynamic and kinetic stability.

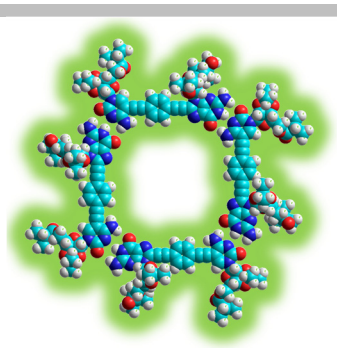

*Carlos Montoro-García, Jorge Camacho-García, Ana M. López-Pérez, Nerea Bilbao, Sonia Romero-Pérez, María J. Mayoral and David González-Rodríguez**

Page No. – Page No.

High-fidelity Noncovalent Synthesis of Hydrogen-bonded Macrocyclic Assemblies